Materials Physics and Mechanics 47 (2021) 621-632 Received: March 31, 2021
Research article

# THERMO-MECHANICAL BEHAVIOR OF THE BEAD WELD OF HIGH-DENSITY POLYETHYLENE (HDPE) PIPES

**A. Belaziz[1*], M. Mazari[2], R. Brahami[1]**

[1]Mechanical Research Center Constantine, University campus of châaberssas, Constantine, 25017, Algeria

[2]Laboratory of Materials and Reactive Systems (LMSR), Mechanical Engineering Department, Faculty of Technology, University of Sidi Bel Abbes, Sidi Bel Abbes, 22000, Algeria

*e-mail: belaziz2013@gmail.com

**Abstract.** The present paper has made it possible to highlight the thermo-mechanical behavior of the bead weld by the butt fusion welding process of two high-density polyethylene (HDPE) pipes. We proposed a welding technic for assembly two plastic pipes to see the effect of fluid pressure and the stress distribution during the welding process at the bead weld. To answer this objective, we wrote a finite element program named D-flux in Fortran95 language [1] then we implemented the (.For) files within the finite element code. The numerical simulation by Finite element makes it possible to evaluate the relevance of the proposed approach and validate the accepted hypotheses for this welding process. This numerical simulation of the thermal cycles of welding was conducted to evaluate the impact of welding on bead weld behavior.

**Keywords:** thermo-mechanical, bead weld, butt fusion, simulation, high-density polyethylene (HDPE) pipes, residual stress

## 1. Introduction

In reality, the butt welded high-density polyethylene (HDPE) pipes are widely used to transport liquid material such as drinking water or natural gas under very high pressure [2]. The residual stress effect on the thermo-mechanical behavior of bead welded has not been quantified sufficiently yet. Current thermo-mechanical behavior standards and recommendations are based on the assumption of yield strength magnitude tensile residual stresses if the actual residual stress state is unknown. It is obvious that information on the number of residual stresses remaining in the bead weld after relaxation, thus acting as mean stress, is highly desirable. The residual stress and hoop stress state in girth-welded pipes differ significantly from the one observed in plates, they are present in materials without any external pressure [3]. and normally result from deformation heterogeneities appearing in the material. The residual stress and hoop stress have a very important role in the strength and service life of bead weld. The estimation of the residual stresses requires separation between the thermo-mechanical Behavior effects and the microstructure.

## 2. Welding Simulation

The butt welding process was simulated using an uncoupled thermo-mechanical finite element analysis using several calculation codes.

Numerically, to obtain a solid and hard weld bead, the welding process by butt fusion requires the application of heat and pressure welding [4]. The heat generated depends on the

http://dx.doi.org/10.18149/MPM.4742021_10

melting temperature, welding pressure, and heating time. The welding resistance depends on the size and shape of the bead, the resistivity of the base material, and its surface condition.
For 3D simulation of the welding process for butt fusion in FEM code, we use a subroutine named D-Flux. The assigned properties are thermal conductivity, specific heat, density, and thermal expansion. These properties are summarized in Table 1.

The equations of the D-Flux model were created by FORTRAN90 and verified by the UMAT [5].

In these models, the moving heat of welding has been applied as a source of volumetric heat and expressed by the following equation:

$$q_r = (x, y, z, t) = \frac{6\sqrt{3} f_f Q}{abc_f \pi \sqrt{\pi}} e^{-x^2/a^2} e^{-3y^2/b^2} e^{-3z^2/c_f{}^2}, \quad (1)$$

where $x, y$ and $z$ – the local coordinates of the model; $Q$ – the power of the welding heat source [w]; $a$, $b$ and $c_f$ – the parameters of the heat source.

Table 1. Properties of HDPE during the merger

| Temperature (°C) | Thermal conductivity (W/m.k) | Specific heat (J/kg.k) | Density (kg/m$^3$) | Thermal expansion ($10^{-5}$/k°) |
|---|---|---|---|---|
| 473.15 | 0.36 | 2000 | 842 | 18 |

In this part, the numerical analysis includes two steps. The first step is to solve the problem of the creation and distribution of residual stress at the bead during the welding process with different environmental temperatures. The second step concerns the variation of the welding pressure in the welding phase. The thermo-mechanical properties of HDPE-/-HDPE pipe welded, such as Young's modulus, Poisson's ratio, the thermal expansion coefficient, and the elastic limit, depending on the ambient temperature (environment) and the welding pressure.

During welding, the heating temperature and the welding pressure can introduce stresses in two directions; residual stresses according to the length of the pipe and circumferential depending on the inside diameter of the pipe.

To verify the equations of D-Flux models by the UMAT [6], we determine the residual stresses of the weld bead during the welding process at different environmental temperatures which are respectively *TD* = 20, 30, 40, 50 and 60°C with a welding pressure *F* = 1400 N and a welding time of 30 minutes.

The 3D finite element model pipe with 32724 elements (Fig. 1), the type of element used in thermal analysis is a biquadratic quadrilateral with 8 nodes of stress-/-/displacement with reduced integration (C3D8R). Due to the axisymmetric FE model around the x-axis and the reduction of the calculation time, half of the model was selected as the analysis model. The y-axis is the contact surface of the two tubes used.

In order to study the thermal behavior of the bead weld, we must determine the distribution of hoop stresses through the pipes during the deformation phases.

Figure 2 shows the distribution of stresses circumferential elasto-plastics through the thicknesses of the pipes studied. With the increasing variety of the pressure interior of the pipes we can see that the first point of plasticity is at $r = a$ when the pressure ($P$) reaches its limit value of elasticity ($P_{lim}$) [7].

From this value, a zone of total plasticity of radius ($c$) develops according to the increase of the internal pressure in the cylinder from which the appearance of a plastic zone and another elastic zone. Indeed it is clear to notify that these stresses are maximum on the interior area of the pipes (Fig. 3).

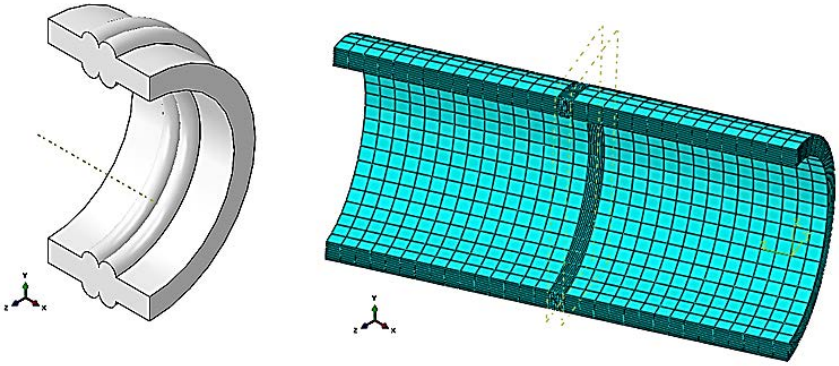

**Fig. 1.** 3D finite element model and the mesh used

The hoop stress is defined in the following form:

$$\sigma_c = \frac{P.D_e}{2t}, \quad (2)$$

where $P$ – applied pressure [bar]; $D_e$ – interior diameter of the pipe [mm]; $t$ – thickness of the pipe [mm].

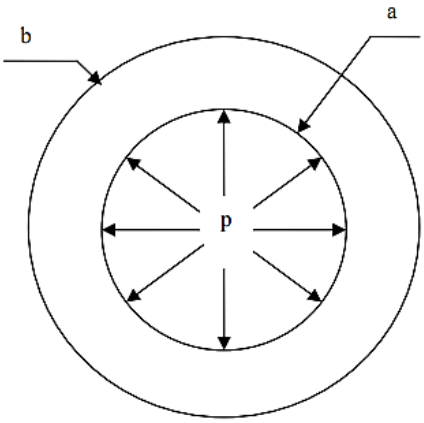


**Fig. 2.** Internal pressure applied in the tube

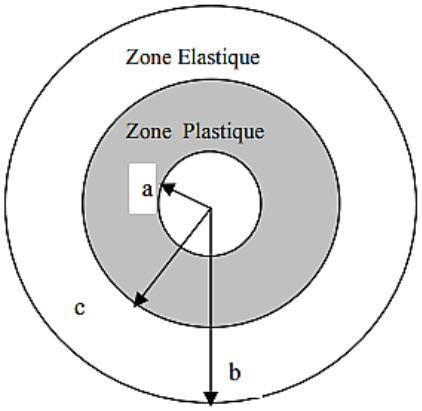


**Fig. 3.** Progression of the plastic zone from the inner surface

The stress intensity factor $K_I$ is a load parameter of a cracked structure that has a significant influence on the analysis of cracked materials.

It is the main parameter of calculation in this study. That is why, from this importance, we were interested in the prevention of fractures in HDPE-/-HDPE welded pipe [8]. For it, another numerical simulation on two cracked structures with the ratio $a / t$ = 0.04 (Fig. 4a) and (Fig. 5a) were realized the two structures have the following dimensions:

Table 2. Dimensions of specimens studied for FIC simulation

| Type of specimen | Interior Diameter (mm) | Thickness $t$ (mm) | Crack length ($a/t$) (mm) |
|---|---|---|---|
| Healthy | 100 | 12.5 | 0.04 |
| Bead | | 17.5 | |

The boundary conditions applied to the pipes during the test are an internal pressure of 4 Bar (40 MPa), a displacement, and a rotation (*U2 = UR2 = 0*) along the y-axis [9]. The application of the axisymmetric model FE on the x-axis is chosen for the reduction of the calculation time (Fig. 4b) and (Fig. 5b).

The choice of the mesh is important for two reasons which will guide its dimensioning. On the one hand, the greater the number of degrees of freedom, the longer the calculation time.

On the other hand, the impact of the mesh which is linked to the precision of the desired result. This means that the smaller the elements, the more the solution announced by the solver approaches the appropriate solution.

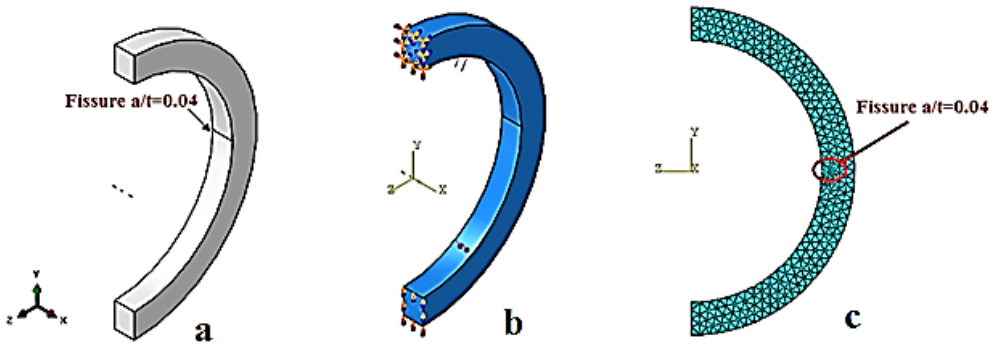


**Fig. 4.** The geometric model, the boundary conditions, and the mesh used for the numerical simulation

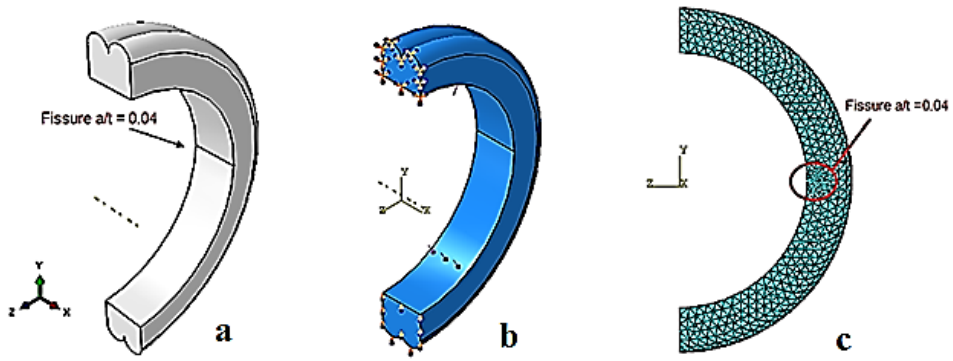


**Fig. 5.**The geometric model, the boundary conditions, and the mesh used for the bead weld

To facilitate the simulation, nonlinear tetrahedral elements with 10 integration nodes were chosen (Fig. 6). These elements are the most used because there are automatic mesh algorithms that allow to completely and quickly discretize a volume while minimizing the number of elements.

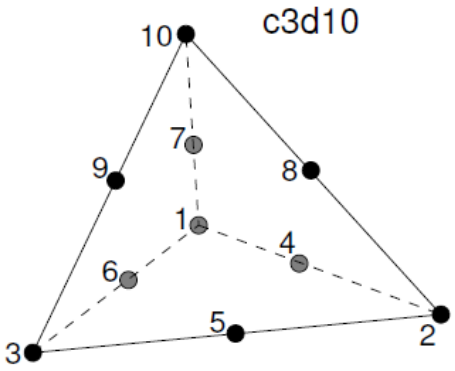


**Fig. 6.** Nonlinear tetrahedral element with 10 integration nodes

The combination of optical microscopy, scanning electron microscopy (SEM), energy-dispersive X-ray spectroscopy (EDS), and X-ray diffraction (XRD) were used to evaluate the properties and behavior of materials. There are two general approaches to model the properties of materials with complex microstructures. One is to use mean-field approximations and to calculate the average properties of a statistically representative microstructure. The second is to accurately model a specific microstructure (or a set of microstructures), using all geometric data available. Although the average field method provide useful bounds for calculating the actual properties and response of materials. The second method is useful in situations where:

- the macroscopic properties area non-linear function of the underlying properties;
- the underlying properties are spatially non-uniform;
- we do not know exactly what properties should be averaged (all molecules of a microstructure (average) have the same shape, orientation, and modulus);
- the properties of interest come from extremes of property distribution (a failure mechanism may depend on the presence of a single point of extreme stress).

In this part, microstructural numerical analysis, the methodology based on the combination of oriented finite elements and a nonlinear finite element, was carried out to determine the elastoplastic properties of the bead weld and briefly discuss some of the most important features of the bead weld. For this, we used a calculation code per element finite OOF2. OOF2 is a program designed to calculate the properties and local behavior of the microstructures of the melted part such as the bead weld. With OOF2, we assigned material properties with characteristics of an experimental or simulated micrograph; generate a finite element mesh from a two-dimensional representation and microstructural images by SEM. This last calculation code can solve a wide range of physical phenomena and can be easily extended.

## 3. Results and Discussion

**Effect of distribution of heat flux on the field residual stresses.** The contour of the temperature during welding is shown in Fig. 7. The flow of heat is not exactly reached at the interface with the heating source [10], but at a distance of a few millimeters. The origin of the residual welding stresses is related to the location of the heat source and the variations of the mechanical properties of a material according to the temperature of environments ($T_D$). The flow limit is very low in high-temperature environments ($T_D$). All the appearing deformations correspond to plastic deformations.

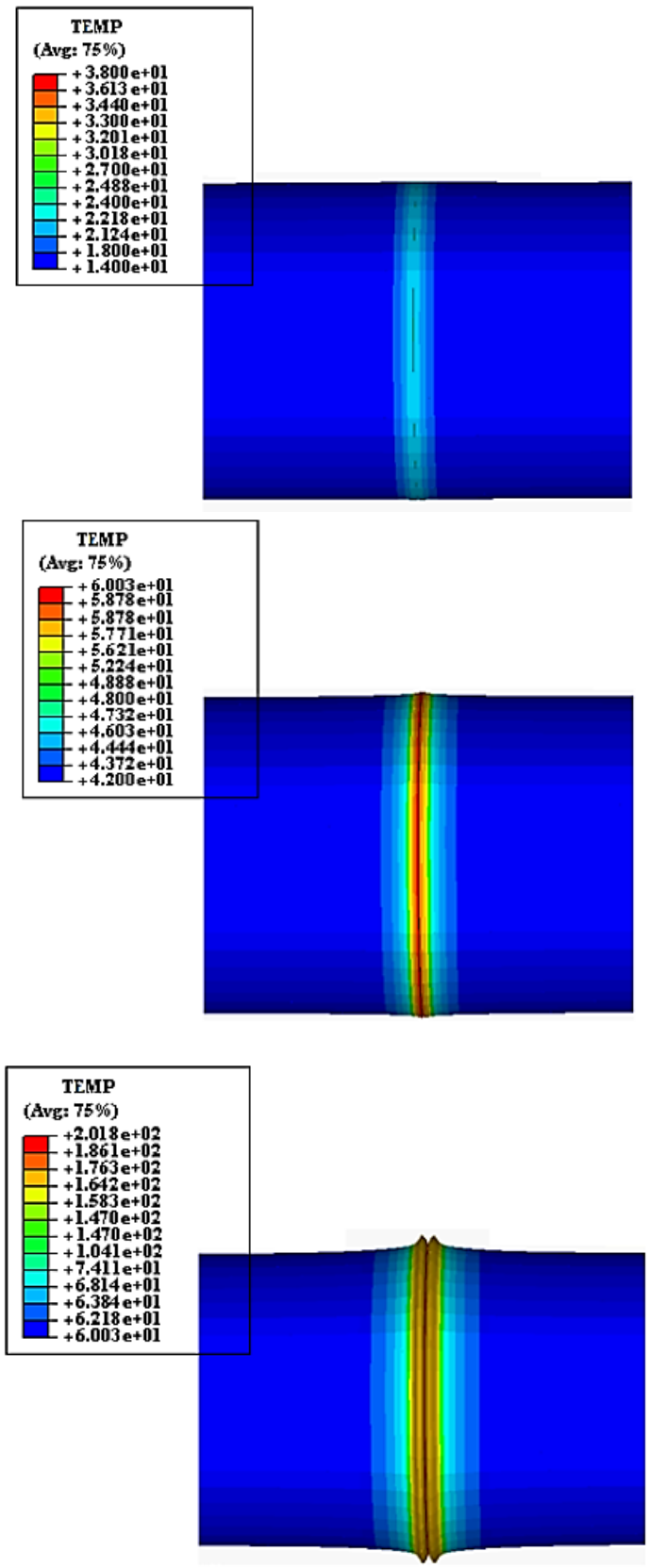


**Fig. 7.** Numerical simulation of the butt fusion process

For different temperature environments ($T_D$), the results of the distribution of the residual stresses obtained during welding are represented in Fig. 8. The melted material

presents good behavior during its spread and during the merger. What made it possible to obtain consolidated materials with good mechanical properties due to residual stresses. We notice that the solder bead presents a significant increase in the flow stress for different environmental temperatures ($T_D$=20, 30, 40, 50, and 60°C). Welding bead presents a fragile behavior at high environmental temperature ($T_D$ =60°C). There is a good concordance between the different temperatures used. We therefore, conclude that the mechanical behavior of the bead depends heavily on the environment temperature and the heating pressure. Indeed an increase in the environmental temperature causes a decrease in the flow stress.

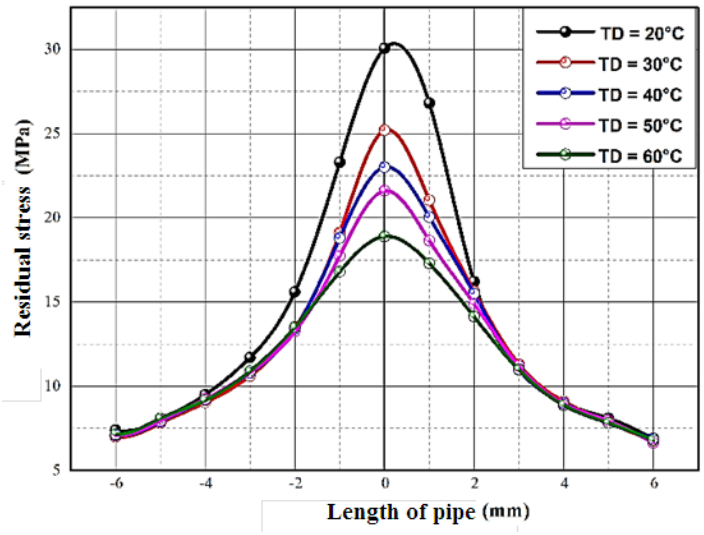


**Fig. 8.** The distribution of residual stresses during butt fusion welding

**Evaluation of the welding pressure on the ambient temperature ($T_D$).** During the welding phase, the material is ejected into the bead that wraps around itself. To follow the variation of the welding pressure at ambient temperatures (environment), a welding force was applied for a welding time of 30 min. The variation of the force applied during the welding time shows that the welding force has several peaks during welding (Fig. 9). The result is interesting because, when the first peak appears, produces a relatively important displacement of matter which proves that at this moment of welding a large welding force of about 950 N and 1150 N is sufficient to advance the tubes and move the matter to the bead.

For an environment temperature $T_D$= 20°C, the profile of the welding force shown in Fig. 9 which reaches 1150 N at the start of welding increases to reach 1200 N.

Table 3 summarizes the results obtained for different environmental temperatures ($T_D$).

Table 3. The effect of environmental temperature (TD) on fusion welding

| Environmental temperatures ($T_D$) (°C) | Peak 1 | | Peak 2 | |
|---|---|---|---|---|
| | Force (N) | Time (min) | Force (N) | Time (min) |
| 20 | 1161.48 | 2.84 | 1205.81 | 28.04 |
| 30 | 1128.98 | 3.42 | 1187.84 | 24.85 |
| 40 | 1025.99 | 3.50 | 1181.41 | 22.35 |
| 50 | 1017.01 | 3.75 | 1030.76 | 20.40 |
| 60 | 969.95 | 3.21 | 1002.98 | 15.84 |

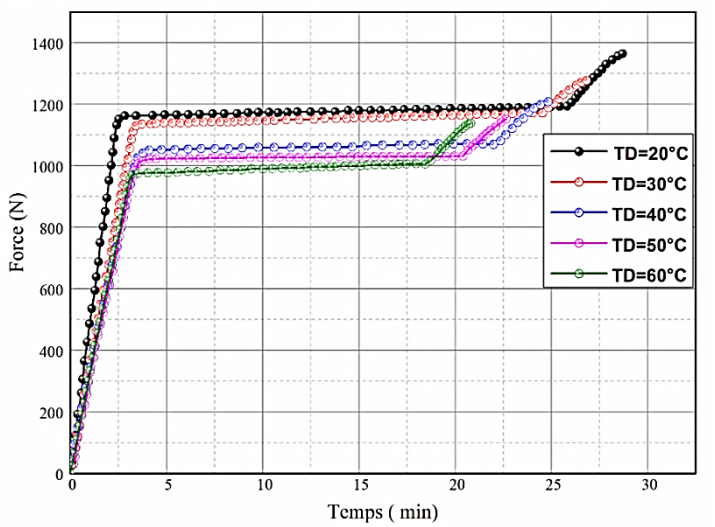


**Fig. 9.** The evaluation of the welding force on the heating time

**Effect of Hoop stress.** Figure 10 shows the results of the distribution of hoop stresses on the inner wall of the pipes for the two cases realized. The results obtained show that during the deformation, the two pipes pass through three phases of deformation: elastic, elastoplastic, and perfectly plastic. In the elastic phase, the hoop stresses of the weld bead are clear, and note that they are maximum on the inner wall of the tube from which the application of internal pressure. In this zone, the hoop stresses are small compared to a healthy pipe. By cons, when the pressure field tends towards the plastic zone hoop stresses decrease until reaching a limited time then gradually increase in the plastic area.

From the results obtained it is concluded that the hoop stresses of the melted part (bead) increase as a function of the enlargement of the plasticity zone. This results in the appearance of residual stresses that have a detrimental effect on the structure of the pipe. This can cause the appearance of cracks or even its break.

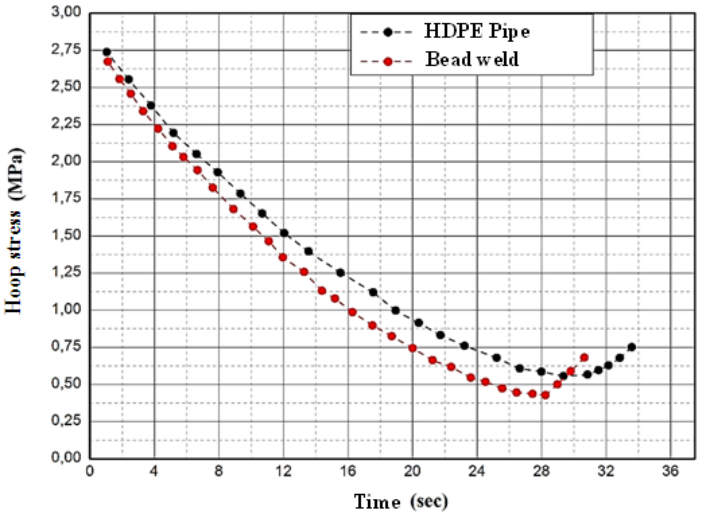


**Fig. 10.** Hoop stress distribution

**Determination of the stress intensity factor $K_I$.** The variation of the stress intensity factor ($K_I$) following the thickness of the pipes used is shown inFig. 11. For the two cases studied, the stress intensity factor ($K_I$) is approximately 1.87 and 0.67 MPa $m^{1/2}$ for the initial cracking of the report ($a/t$ =0.04). On the basis of this result, we can suppose, for the next two

simulations, that the crack starts from the same crack front. For a short crack, the presence of the bead weld in the pipe causes a small increase in the stress intensity factor relative to the healthy pipe. This increase is the result of the stress concentration in the notch where the crack starts. In addition, the stress intensity factor also decreases with the advancement of the crack according to the thickness of the pipe. For longer cracks, the stress intensity factor is similar to that obtained in the study of the healthy pipe. It can be seen that the stress concentration in the welded part has a significant impact on the initiation of the radial crack. The value of the stress intensity factor for a healthy ring is shifted higher than the ring with solder. The change in material properties in the welded zone (bead) is mainly caused by changes in crystallinity. In the case of HDPE-/-HDPE pipe welded, for reasons of changes in spherulitic morphology, the effect of the stress intensity factor on the crack is important.

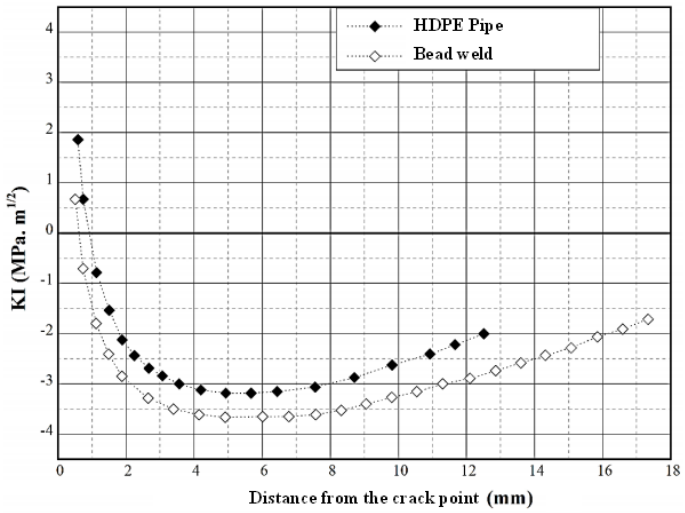


**Fig. 11.** Evolution of the stress intensity factor for the two pipes used

**Microstructural analysis.** For the simulation of microstructures by OOF2, three independent steps. In the first step, the cross-sections are taken a welded tube and the bead part identifies microstructural images per microscopy Scanning electron SEM (Fig. 12).

In the second step, microstructural images are imported into the finite element analysis program OOF2 for segmentation and mesh (Fig. 13). The final step examines the microstructural structures to determine the elasto-plastic properties of the bead weld and to visualize the microscopic microstructure response to external conditions.

The Table 4 summarizes the results of the main mechanical properties for different periods of exposure. From to these results, the numerical microstructure analysis of images, we indicated that there are small remarkable variations of the modulus of elasticity ($E$) and Poisson's ratio ($v$). In this part, the mechanical properties are determined in pixels in a very small range with a well-refined mesh. These results have a very reliable ductility at the ambient temperature used (Fig. 14). The mechanical properties of the bead weld strongly depend on the parameters of the microstructure.

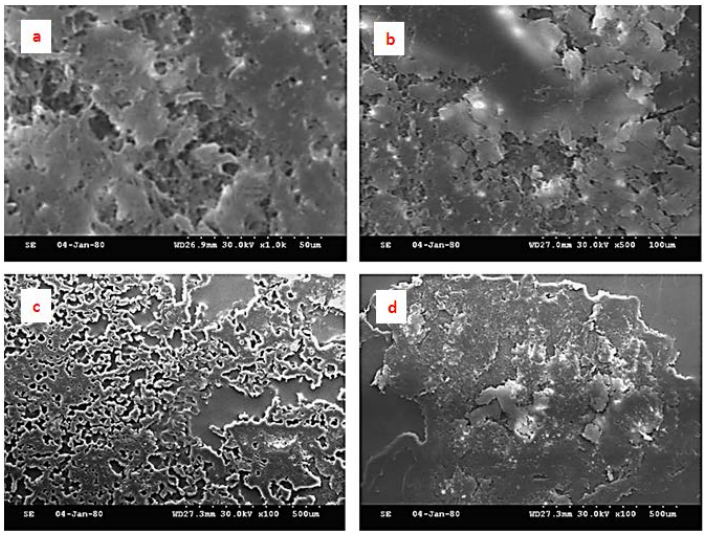


**Fig. 12.** Identification phase of the microscopic image by scanning electron microscopy (SEM) [11]

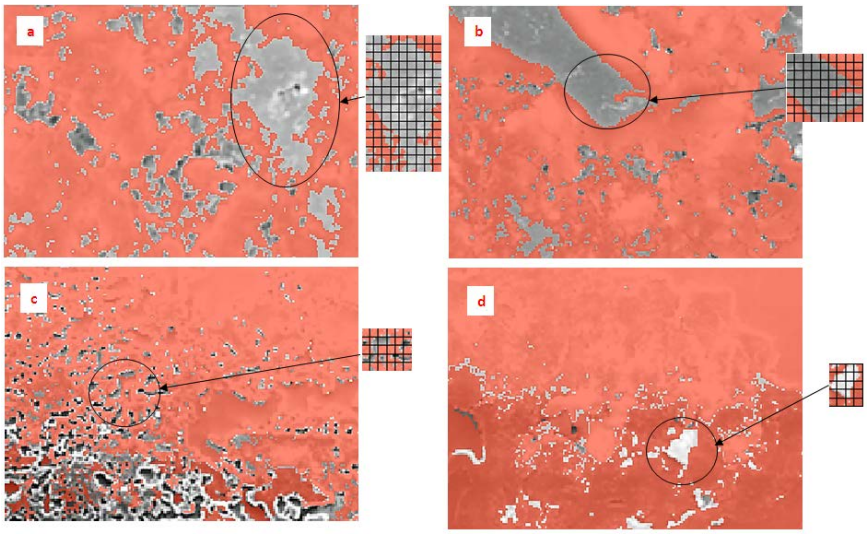


**Fig. 13.** Segmentation phase and mesh

Table 4. Comparison between the mechanical characteristics for different positions on the microstructure of the bead

| Measurement image | Number of elements | Number of Nodes | Young's module *E* (MPa) | Poisson's ratio *v* |
|---|---|---|---|---|
| a | 1645 | 1792 | 780 | 4393E-4 |
| b | 1610 | 1728 | 771 | 4375E-4 |
| c | 1583 | 1662 | 756 | 4323E-4 |
| d | 1531 | 1601 | 742 | 4309E-4 |

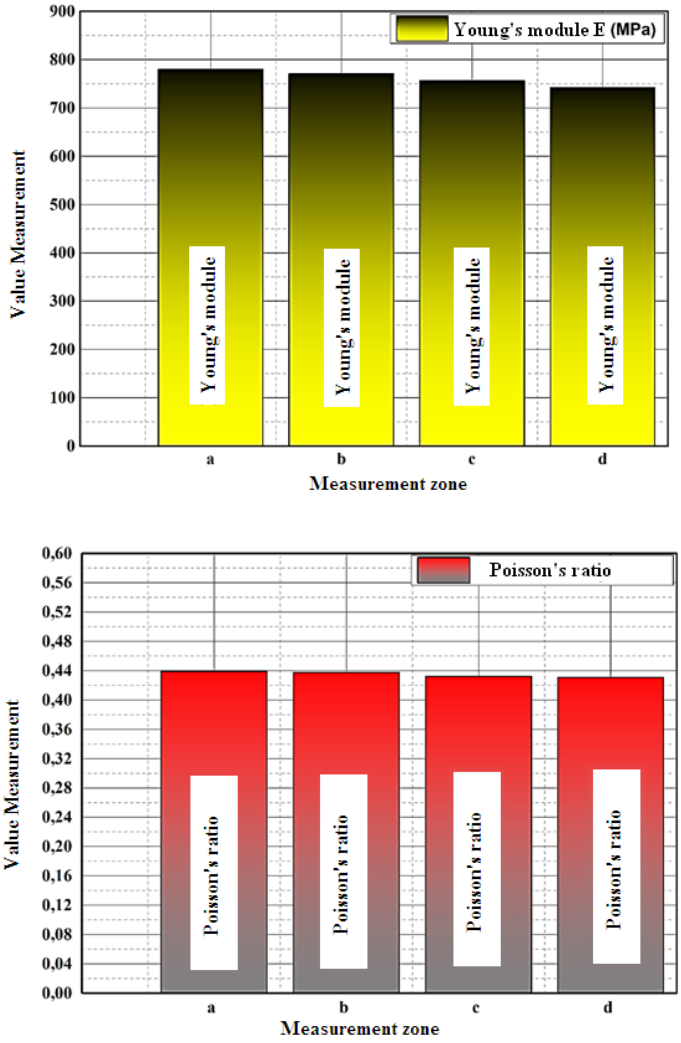


**Fig. 14.** Variation of modulus of elasticity and Poisson's ratio for different positions on bead microstructure

## 4. Conclusions

This work reports one of the first comprehensive 3D simulations of the residual stresses, the hoop stress, and the stress intensity factor $K_I$ in the bead weld of the thick section in HDPE pipes. The work will serve as one of the few high-quality numerical data that can be used to develop and finite element models for predicting residual stresses and the hoop stress in bead weld of High-Density Polyethylene (HDPE) Pipes. The results of this paper show that:

- In bead weld the effect of the distribution of heat flux on the field residual stresses is very complex and sensitive to the distance from the weld centerline, the residual stresses were asymmetric, which was attributed to the constraints induced by weld pass sequence across the weld groove. Residual stresses were strongly compressive to the weld center.
- Numerically, As the bead welds are made in the 'solid state' they are difficult to inspect but there are thermal effects on the parts being welded. Changes in ambient temperature ($T_D$) affect the quality of Bead Weld of High-Density Polyethylene (HDPE) Pipes.
- Residual stress near the outer surface is more sensitive to the distance from the bead weld centerline. The numerical analysis of obtained results may be concluded that

the factors with significant influence on the quality of bead welded are environment temperature and welding time, whereat welding time has the strongest influence.

In microstructural analysis, estimates of Young's modulus and Poisson's ratio are obtained in different zones, use finite element numerical simulation. Uncovering accurate mechanical properties such as Young's modulus, Poisson's ratio, have become critical factors for making research and design of engineering materials.

***Acknowledgements.*** *No external funding was received for this study.*

**References**

[1] Abburi KV, Kumar S, Dey HC, Smith DJ, Bouchard PJ and Truman CE. Study on the Effect of Post Weld Heat Treatment Parameters on the Relaxation of Welding Residual Stresses in Electron Beam Welded P91 Steel Plates. *Procedia Engineering.* 2014;86: 223-233.
[2] Dean D, Hidekazu M. Prediction of welding residual stress in multi-pass butt-welded modified 9Cr–1Mo steel pipe considering phase transformation effects. *Computational Materials Science.* 2006;37(3): 209-219.
[3] Xu J, Jia X, Fan Y, Liu A, Zhang C. Residual Stress Analyses in a Pipe Welding Simulation: 3D Pipe Versus Axi-symmetric Models. *Procedia Materials Science.* 2014;3: 511-516.
[4] Prasad VMV, Varghese JVM, Suresh MR, Kumar DS. 3D simulation of residual stress developed during TIG welding of stainless steel pipes. *Procedia Technology.* 2016;24: 364-371.
[5] Oden JT, Kikuchi N. *Finite Element Methods for Constrained Problems in Elasticity.* TICOM. University of Texas at Austin. Austin. Texas. 1980.
[6] Karlsson H, Sorensen I. *ABAQUS/Standard user's manual Providence. Rhode Island.*
[7] Azzeddine B, Mazari M. Experimental Study of the Weld Bead Zones of a High-Density Polyethylene Pipe (HDPE). *Journal of Failure Analysis and Prevention.* 2018;18(2): 1-12.
[8] Azzeddine B, Mazari M. Experimental and Numerical Study of Bead Welding Behavior of HDPE Pipe Under Uniaxial Loading. *Mechanics and Mechanical Engineering.* 2019;23: 183-191.
[9] *ABAQUS Manual*. 1989. version 4.8.
[10] Kwon HJ, Jar PYB. On the application of FEM to deformation of high-density polyethylene FEM. *International Journal of Solids and Structures.* 2008;45: 3521-3543.
[11] Pashupati P, Yoonsang K, Sunwoong C. Microstructure and Mechanical Properties of the Butt Joint in High Density Polyethylene Pipe. *Internationa Journal of Polymer Science.* 2016;16: 1-13.